TECHNISCHE MECHANIK, Band 22, Heft 3, (2002), 193-204
Manuskripteingang: 10. Juli 2001

Decoupling of Mechanical Structures with Piezoceramic Stacks

S. Herold, D. Mayer, H. Hanselka

A review of the development and realisation of an adaptive interface for decoupling of two mechanical systems is presented. An approach is utilized to design an adaptronical system by means of rapid-prototyping on the basis of a simulation. The method includes the calculation of the dynamic behaviour of the mechanical structure with the help of FEM. The FE-model of the mechanical structure is reduced and embedded as modal state-space-model with the numerical simulation software MATLAB/ Simulink. Actuators and sensors are integrated into the mechanical structure. Based on the resulting dynamical behaviour of the mechanical structure an adaptive control algorithm for the decoupling of structural vibrations is developed. Experimental tests are performed to confirm and to update the simulations. The hardware-in-the-loop-simulation is performed with the commercial rapid-prototyping dSpace-system. This procedure allows the development and the evaluation of more complex adaptive mechanical structures.

1 Introduction

Efficient use of traditional materials results in light weight structures with a small mass-to-stiffness-ratio. In consequence, larger mechanical vibrations occur. Recently, smart materials have been developed for the suppression of these vibrations. They can carry mechanical loads and additionally operate as sensors and actuators. To prevent the propagation of vibrations through various mechanical structures is the main subject of this work.

It is necessary to apply forces at the linkage of the coupled structures, for which an adaptive interface (Bein and Lammering, 1995) based on piezoceramic actuators is considered. It is able to transmit static forces while isolating dynamical disturbances. The adaptive interface is mounted on a bi-clamped beam and driven by a digital controller in such a way that no dynamical disturbing forces act on the beam. First of all the dynamical behaviour of the beam is computed with the help of FEM (Bathe, 1990). The FE-model of the mechanical structure is reduced subsequently and integrated as a modal state-space-model in the MATLAB/ *Simulink*-environment. Actuators and sensors are embedded into the model. An adaptive control algorithm (Kuo and Morgan, 1996) for the decoupling of structural vibrations is also integrated in the MATLAB/ *Simulink*-environment. Experimental tests with a hardware-in-the-loop-simulation show the efficiency of the controller in reality. The experiments are performed with the help of a dSpace-system.

2 Analytical Model

The construction of the adaptive interface includes two piezoceramic tube actuators, a screw, and four PVC-washers (Figure 1). The tube actuators are working against each other, i.e. one actuator is contracting, while the other is expanding, causing a relative motion between the two structures. Hence, the pre-stress in the interface remains constant. Forces on the structures can only be applied in normal direction. In this work, for simplicity, one structure is a bi-clamped beam, while the other is the head of the screw (Figure 2).

The steel-beam ($300\times30\times2$ mm^3, E = 210000 N/mm^2, ν = 0.3, ρ = 7850 kg/m^3) is modelled with two sections, where the force of the actuators, damping and spring forces are applied as boundary conditions. Therefore a system of three coupled differential equations of motion exists. The interface is modelled as an 1 DOF mass-damper-spring system ($c = 10^8$ N/mm, m = 0.0614 kg). The stiffness c of the actuators is taken from the manufacturers specification. The mass m represents the mass of the actuators, the mass of the impedance head and the mass of the screw head.

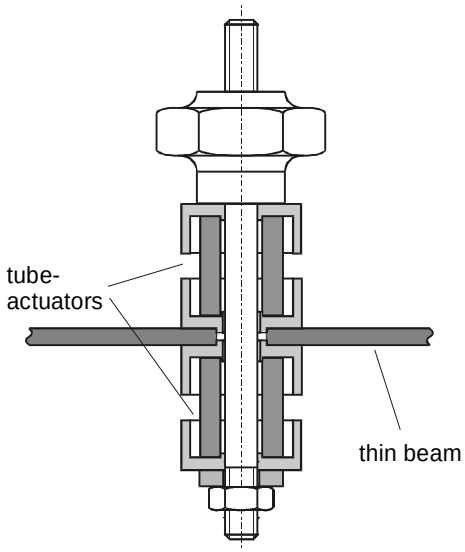

Figure 1: Adaptive Interface

The disturbing force F_s acts on the interface model on the rigid mass m. Stiffness c and damping coefficient d are inherent parameters of the actuators. The actuator force F_P is driven by a digital controller. The equation of motion of the beam and the interface are shown in equation (1).

$$\begin{aligned} &EI_{yy} w_{1,x_1x_1x_1x_1} + \rho A \ddot{w}_1 = 0 \\ &EI_{yy} w_{2,x_2x_2x_2x_2} + \rho A \ddot{w}_2 = 0 \\ &-m\ddot{w}_3 + d\,(\dot{w}_2(x_2 = 0) - \dot{w}_3) \\ &\qquad + c\,(w_2(x_2 = 0) - w_3) + F_P = -F_S \end{aligned} \tag{1}$$

with the displacements w_i shown in Figure 2. The stiffness of the continuous beam model is expressed by the product of Young's modulus E and moment of inertia I_{yy}, while the mass of the beam is described by the product of density ρ, cross-sectional area A and the length l of the beam.

All boundary conditions for the whole mechanical system are explained in the following expression:

$$\begin{aligned} &w_1(x_1 = 0) = 0 \quad ; \; w_{1,x_1}(x_1 = 0) = 0 \\ &w_2(x_2 = l_2) = 0 \quad ; \; w_{2,x_2}(x_2 = l_2) = 0 \\ &w_1(x_1 = l_1) = w_2(x_2 = 0) \quad ; \; w_{1,x_1}(x_1 = l_1) = w_{2,x_2}(x_2 = 0) \\ &E_1 I_1 w_{1,x_1x_1}(x_1 = l_1) = E_2 I_2 w_{2,x_2x_2}(x_2 = 0) \\ &E_1 I_1 w_{1,x_1x_1x_1}(x_1 = l_1) = E_2 I_2 w_{2,x_2x_2x_2}(x_2 = 0) - c\,(w_2(x_2 = 0) - w_3) - d\,(\dot{w}_2(x_2 = 0) - \dot{w}_3) - F_P \end{aligned} \tag{2}$$

The mechanical systems analysed here are lightly damped, so that the damping can be neglected for eigenvalue computation (resulting in real eigenvectors). Using equation (2) with the approximation function (3) yields a linear system of equations (4). **K** is the system matrix, **A** the vector of unknown coefficients and **F** is the force vector. To compute the eigenvalues of the system the zeros of the determinant of the system matrix **K** are determined.

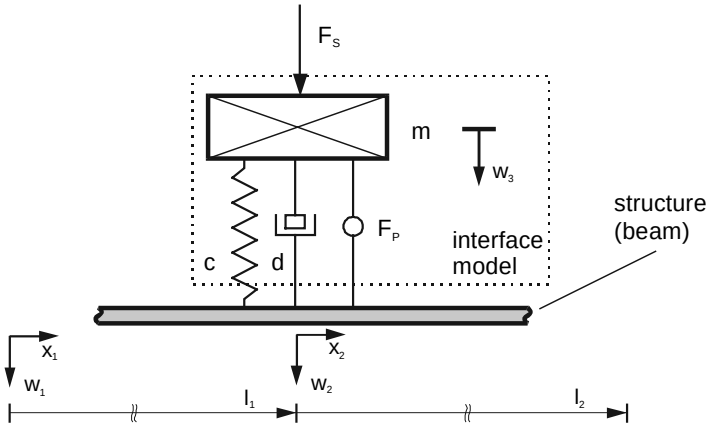

Figure 2: Model of the Mechanical System

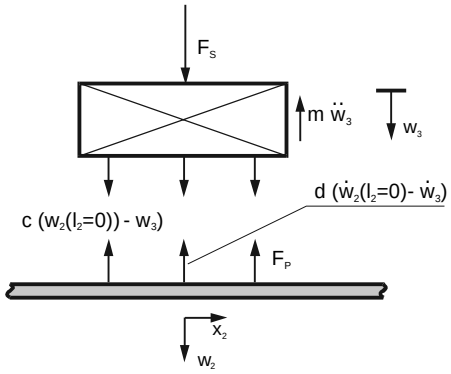

Figure 3: Forces Acting on the Analytical Interface Model and Boundary Conditions between the First and Second Section of the Beam

$$w_i = A_{1i}\sin(\lambda x_i) + A_{2i}\cos(\lambda x_i) + A_{3i}\sinh(\lambda x_i) + A_{4i}\cosh(\lambda x_i) \qquad i = 1,2$$
$$w_3 = A_5 \tag{3}$$

$$\mathbf{KA} = \mathbf{F} \tag{4}$$

For solving the eigenvalue problem of this system the program Maple V is used. λ are the eigenvalues of the structure. The first five eigenfrequencies (Table 1) of the whole system are computed. The harmonic response function can be determined by solving equation (4) with a sinusoidal exciting function $f = \hat{f}\sin(\Omega t)$ in the force vector **F** with discrete frequency steps.

Table 1. Eigenfrequencies of the Mechanical System

	f_1 [Hz]	f_2 [Hz]	f_3 [Hz]	f_4 [Hz]	f_5 [Hz]
Analytical Solution	89.61	224.5	537.0	1017	1511

For decoupling the two structures, a feedforward control algorithm is considered. To calculate the optimal control force in the frequency domain, (1) is transformed into Fourier space. As a second equation, the mobility at the interface mounting point on the beam is calculated from the velocity of the beam and the force acting on it. Decoupling of the two structures is guaranteed if w_2 vanishes at the mounting point. Assuming the modal superposition principle of vibration, the vibration of the whole beam should be prevented. Solving the set of equations for F_p, the optimal control force is received (see (Hansen and Snyder, 1997), pp. 1118):

$$M(j\omega) = \frac{j\omega w_3}{F_p(j\omega) + c\,(w_2 - w_3) + j\omega\, d\,(w_2 - w_3)}$$

$$F_p(j\omega) = F_s(j\omega)\frac{(c + j\omega\, d)}{\omega^2 m} \tag{5}$$

3 Finite Element- and MATLAB/*Simulink*- Model

With the help of the FE-system COSAR a structural model of the bi-clamped beam is generated. Semiloof-shell elements (8-nodes) with quadratic displacement functions are applied. Shell elements are used to have the possibility of expanding the method to more complicated structures (e.g. cylindrical structures). A fine mesh is used to resolve higher order modes (Figure 3). The FE-model is described by following differential equation (6) for the undamped system and boundary conditions (7). For lightly damped structures the damping can be neglected for the computation of eigenfrequencies and eigenvectors (resulting in real eigenvectors).

$$\mathbf{M}\,\ddot{\mathbf{w}} + \mathbf{C}\,\mathbf{w} = \mathbf{0} \tag{6}$$

$$\begin{aligned}
&\mathbf{w}(x_1 = 0, 0 \le x_2 \le l_2, t) = 0 \\
&\mathbf{w'}(x_1 = 0, 0 \le x_2 \le l_2, t) = 0 \\
&\mathbf{w}(x_1 = l_1, 0 \le x_2 \le l_2, t) = 0 \\
&\mathbf{w'}(x_1 = l_1, 0 \le x_2 \le l_2, t) = 0
\end{aligned} \tag{7}$$

In equation (6) **M** is the mass matrix, **C** the stiffness, and **w** the vector of coordinates. The numerical modal analysis of the beam supplies eigenvectors and eigenfrequencies (Szabó, 1985).

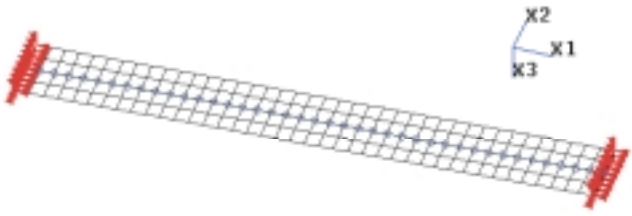

Figure 4: FE-Model of the Beam with Boundary Conditions and Description of the FE-Nodes for the *Simulink*-Export

The adaptive interface (Figure 1) can apply forces to the structure only in normal direction. Therefore, only bending modes of the beam are taken into account to reduce the model size.

It is difficult to export huge models with many degrees of freedom into the MATLAB/*Simulink*-environment. Thus it is necessary to reduce the order of the model by means of modal transformation (Fischer and Stephan, 1993) and choosing only the main DOF's for the description of the bending modes. The result is shown in equation (8), with modal coordinates z_k, the modal damping coefficients ϑ_k, and the eigenfrequencies ω_{k0} .

The forces at the right side of equation (8) are also transformed into the modal space (Fischer and Stephan, 1993).

$$\ddot{z}_k + 2\,\vartheta_k\,\omega_{k0}\,\dot{z}_k + {\omega_{k0}}^2\,z_k = \mathbf{x_k}^{\mathbf{T}}\,f \tag{8}$$

The degrees of freedom for a sufficiently accurate description of the model are chosen (Figure 4) to be $n = 12$ in modal space remain. For a constant spectrum of exciting forces the amplitudes of higher modes are very small and their eigenfrequencies are very distant to the interesting frequency range, in that way the higher modes ($n > 12$) are neglected.

The eigenvectors are reduced from 569 nodes with 2435 DOF to 41 geometrical nodes with 12 modal DOF. The resulting model is exported into the MATLAB-environment in a state-space-formulation (9).The following equations show the system matrices in the modal state-space (Unbehauen, 1994):

$$\begin{aligned}
&\dot{\zeta}(t) = \overline{\mathbf{A}}\,\zeta(t) + \overline{\mathbf{B}}\,\mathbf{u}(t)\\
&\mathbf{y}(t) = \overline{\mathbf{C}}\,\zeta(t) + \overline{\mathbf{D}}\,\mathbf{u}(t)\\
&\zeta(t) = \begin{pmatrix}\dot{\mathbf{z}}\\ \mathbf{z}\end{pmatrix}_{2n}\ ;\ \mathbf{y}(t) = \mathbf{y}(t)_{2n}\ ;\ \mathbf{u}(t) = \mathbf{u}(t)_{2n}\\
&\overline{\mathbf{A}} = \begin{pmatrix}-\mathbf{b} & -\boldsymbol{\omega}^{\mathbf{2}}\\ \mathbf{e} & \mathbf{0}\end{pmatrix}_{2n,2n} \qquad ;\ \mathbf{b} = diag\left(2\vartheta_k\omega_k\right)_{n,n}\\
&\qquad\qquad\qquad\qquad\quad \mathbf{e} = \mathbf{E}_{n,n}\\
&\overline{\mathbf{B}} = \begin{pmatrix}\boldsymbol{\omega}^{\mathbf{2}} & \mathbf{0}\\ \mathbf{0} & \mathbf{0}\end{pmatrix}_{2n,2n} \qquad ;\ \boldsymbol{\omega}^{\mathbf{2}} = diag\left({\omega_k}^2\right)_{n,n}\\
&\qquad\qquad\qquad\qquad\quad \overline{\mathbf{C}} = \mathbf{E}_{2n,2n}\ ;\ \overline{\mathbf{D}} = \mathbf{0}_{2n,2n}
\end{aligned} \tag{9}$$

The modal transformation (forward and backward) is performed in every time step of the simulation outside the state-space model (Figure 6). The submodel “modal model (beam)” in Figure 5 is expanded in Figure 6 to explain the mechanism of modelling more detailed.

The model of the adaptive interface (Figure 2) is integrated as a 1 DOF system, which is modelled in the state-space. Figure 5 shows the realisation of the mechanical part of the adaptive interface in *Simulink*.

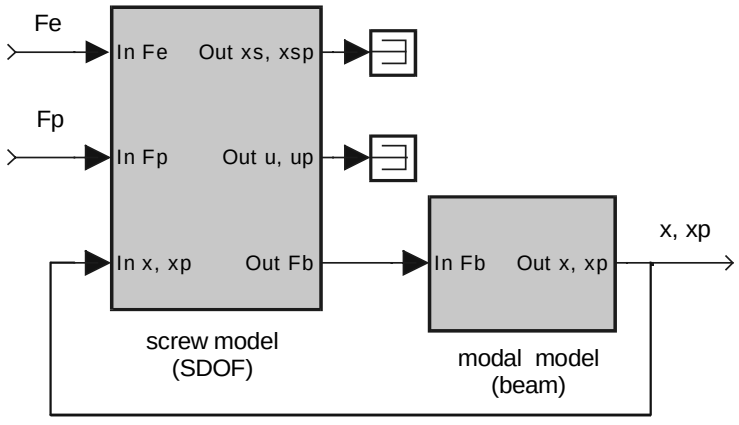

Figure 5: Mechanical System in *Simulink* (F_e-Exciting Force, F_b-Force Acting on the Beam, F_p-Actuator Force)

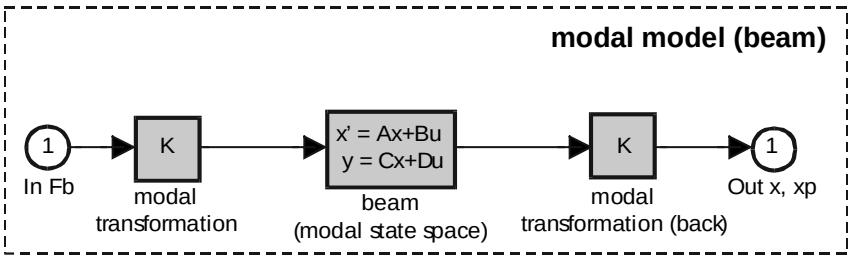

Figure 6: Scheme of the Modal Modelling of the Beam in *Simulink*

A Runge Kutta fourth order algorithm implemented in *Simulink* with a time step size of t_s = 5e-5 s is used to perform the numerical simulations.

The set-up of the model allows an easy replacement of the *Simulink* blocks by the real mechanical structure in case of a hardware-in-the-loop-simulation.

4 Concept for Signal Processing

An adaptive feedforward-controller is implemented to drive the actuators of the adaptive interface (Kuo and Morgan, 1996). This allows automatic adjustment of the control forces to changing physical parameters (e.g. temperature or static mechanical loading) by adaptation of the control filter while observing the vibrations of the beam. The required reference signal is taken from the structure, which is transmitting the vibrations (here: the rigid mass). The error sensor is mounted to the structure, which has to be decoupled (here: the beam), and provides the error signal *e(n)*. Figure 7 shows the block diagram of the adaptronical system. *P(z)* represents the primary path from the disturbance source to the error sensor, where *S(z)* represents the secondary path from the actuator to the error sensor. Since the actuators have an effect on the vibration of the rigid mass, this feedback has to be taken into account with a feedback path *F(z)* from the actuator to the reference sensor on the rigid mass.

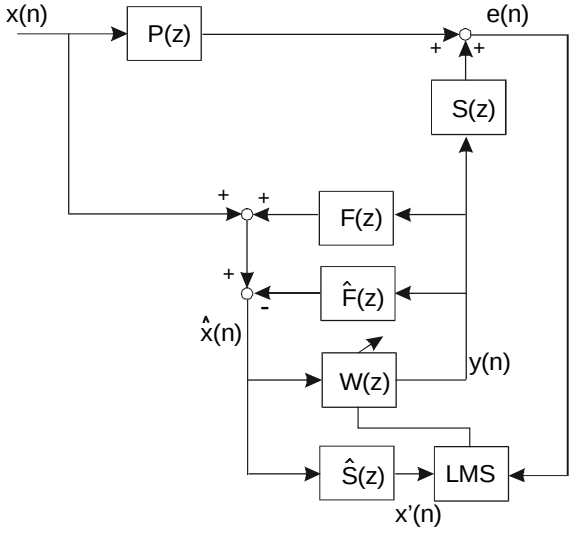

Figure 7: Block Diagram of the Adaptronical System

$\hat{S}(z)$ and $\hat{F}(z)$ are models of these transfer functions. The reference signal $\hat{x}(n)$ is filtered with an adaptive FIR (finite impulse response) filter of order m = 400 to generate the actuator signal *y(n)* (Figure 8):

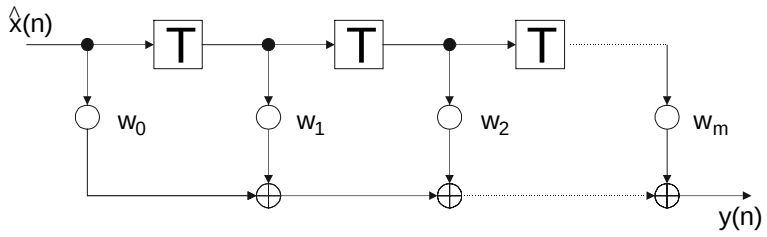

Figure 8: Signal Flow of the Finite Impulse Response Filter *W*

The coefficients $\underline{w}$, which represent the impulse response of the filter *W(z)*, should be adapted in order to minimise the cost function (10), which represents the power of the error signal.

$$\xi = E\{e^2(n)\} \tag{10}$$

A steepest descent method can be implemented by the following adaptation algorithm:

$$\underline{w}(n+1) = \underline{w}(n) - \frac{\mu}{2}\,\underline{x}'(n)\,\frac{\partial \xi(n)}{\partial \underline{w}(n)} \tag{11}$$

To simplify the calculations by the signal processor, the algorithm can be simplified to the so-called stochastic gradient filtered-X-LMS (filtered-X-least mean squares) algorithm (Widrow and Stearns, 1985):

$$\underline{w}(n+1) = \underline{w}(n) + \mu\;\underline{x}'(n)\,e(n) \tag{12}$$

The vector $\underline{x}'(n)$ stores the last *m* values of the reference signal filtered with $\hat{S}(z)$, *e(n)* is the error signal and μ the convergence factor. Favourable characteristics of the F-X-LMS are the usage of stable FIR filters, the unimodal perfomance surface and the unimportance of initial values for the coefficients.

For proper convergence of the algorithm, an independent reference signal without feedback from the actuator is needed. Therefore the actuator signal *y(n)*, filtered with a model of the feedback path $\hat{F}(z)$, is subtracted from the reference sensor signal. In the ideal case of the identity of $\hat{F}(z)$ and *F(z)*, the input signal for the adaptive filter is independent of the actuator signal (Kuo and Morgan, 1996).

The absolute value of the filtered reference signal *x'(n)* still depends on the absolute value of the disturbance signal *x(n)*. Because the convergence behaviour of the simple LMS algorithm depends on the magnitude of its reference signal, it is mostly suitable for artificial reference signals from a signal generator. Since in this application a vibrational reference sensor is used, the magnitude of the received signal may change. Therefore the normalised LMS-algorithm (Kuo and Morgan, 1996) with a variable step size $\mu(n)$ is implemented, which depends on the average power of the *x'(n)*:

$$\mu(n) = \frac{\alpha}{mP_x} \quad \text{where } 0 < \alpha < 2 \tag{13}$$

A recursive process estimates the power of the signal:

$$P_x(n) = P_x(n-1)\,(1-\beta) + \beta\,x'^2(n) \tag{14}$$

This method implements a low-pass filtering of the squared input signal *x'(n)* with the filter time constant β, which is also known as a forgetting factor. It is chosen as $1/m$, so the power is approximately averaged over the last *m* values, but computational costs are substantially lower than for implementation of a moving average (MA) process of order *m*. The convergence and the input signal of the adaptive filter are therefore independent of the disturbance and actuator signal. The models $\hat{S}(z)$ and $\hat{F}(z)$ of the transfer functions *S(z)* and *F(z)* are implemented by adaptive FIR filters, too. Because the impulse responses of the considered system are short enough, a representation with FIR filters is feasible. Before starting the experiments, the system will be identified by white noise (Figure 9):

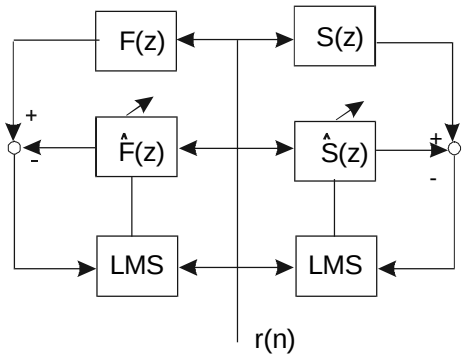

Figure 9: System Identification

The coefficients are adapted in the same way like *W(z)* with the LMS algorithm. The difference of the outputs of the mechanical transfer functions and their models is used as the error signal. The test signal *r(n)* is stochastically independent of the disturbance signal *x(n)*, so an online adaptation for the model of *S(z)* is possible (Kuo and Morgan, 1996). Feedback prevents this for *F(z)*. If the interface is mounted to lightly damped systems, impulse responses of the paths may become too long to be represented with FIR filters, so adaptive IIR (infinite impulse response) filters would have to be used.

The existing simulation of the mechanical system in the *Simulink* environment is completed by the signal processing part. Beside the digital signal processing subsystem described previously, the analog subsystem is modelled. The main parts are the conditioning amplifiers for the sensors, the power amplifiers for the actuators, the ADC and the DAC units with anti-aliasing and reconstruction low passes. The sampling frequency for the analog and the mechanical subsystem is chosen higher than for the digital subsystem, in order to model the former part properly and to chose a realistic sampling rate for the latter part.

First of all, the digital filters are coded with *Simulink* standard blocks for simple testing of various algorithms. Afterwards, the filters are reprogrammed in C and embedded as blocks in *Simulink*, thus the speed of the simulation increases as well as the code for the signal processor becomes more efficient.

Table 2. Comparison of the Simulation with Analytical Solutions

f [Hz]	F_P [N] Calculated	F_P[N] Simulated	Reduction [dB] Simulated
89.7	5760	5680	45
223.9	924	923	54
531.3	164	164	46
1003.8	46	42	14
1499.5	21	20	23

The simulation of the adaptronical system is tested by comparing results for the control force with the ones calculated from (2). As a test case the system is excited in the eigenfrequencies with a sinusoidal force F_S = 1N, and the controller adapts 10 s in order to minimise the error signal.

As shown in Table 2, the simulation agrees well to the analytical results, even if the reduction in the fourth eigenfrequencies is smaller than for the others. The reason for this is that the adaptive interface is mounted near to a node of the corresponding eigenform, so the secondary path has a zero for this frequency and control is nearly impossible.

5 Experiments

Table 3. Used Equipment

Unit	Denotation
DSpace system	MP-system DS 1003 / 1004
Highvoltage-amplifier	PI-HVPZT
Bandpassfilter, reconstructionfilter	Kemo
Electrodynamical exciter	Tira
Impedance head	Brüel & Kjaer
Accelerometer	Brüel & Kjaer
Integrating charge amplifier	Brüel & Kjaer

The mechanical system consists of a bi-clamped steel beam (300×30×2 mm^3). The interface is mounted to the beam at a distance of 75 mm to the edge. The complete configuration with all sensors and actuators is presented in Figure 11. The accelerometer signals are conditioned by charge amplifiers for the DAC. The output signals of the dSpace system, which is used for digital signal processing, are filtered by low passes for reconstruction (Figure 10).

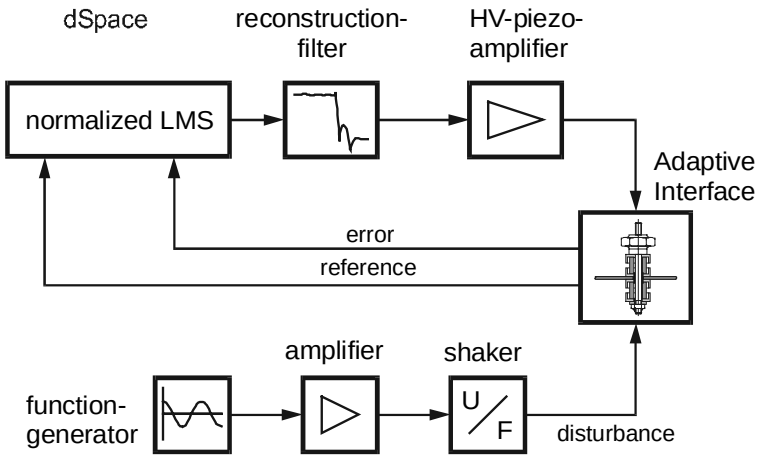

Figure 10: Experimental Set-Up of the Adaptronical System

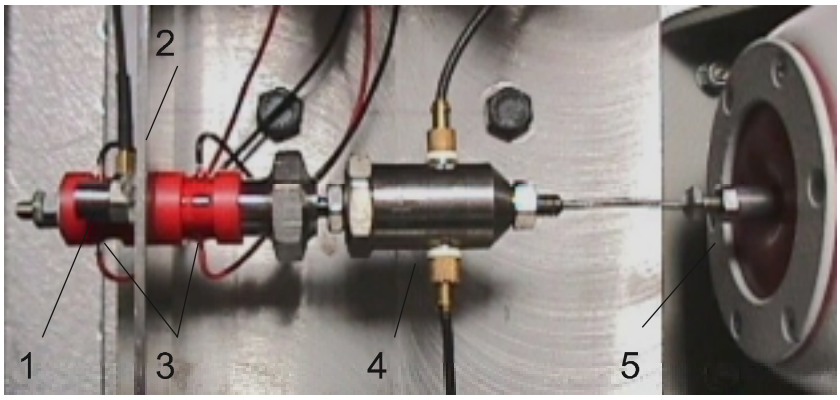

Figure 11: Experimental Set-Up of the Adaptive Interface
(1-Errorsensor, 2-beam,3-piezoceramic tube actuators,
4-impedance head, 5-shaker)

Performed Experiments

The purpose of the experiment is to cancel the beam vibrations in the frequency range from 30 Hz to 800 Hz, including the first three eigenfrequencies of the system.

Experimental Modal Analysis (EMA)

The eigenfrequencies, eigenmodes, and modal damping coefficients of the system without the interface (only the beam) are identified to allow a comparison with the FE-analysis:

Table 4. Comparison between Analytical, Numerical and Experimental Results of Modal Analysis

	f_1 [Hz]	f_2 [Hz]	f_3 [Hz]	f_4 [Hz]	f_5 [Hz]
Analytical solution	116.7	321.8	630.8	1043	1558
FEM	118.2	325.7	639.0	1058	1583
EMA	115.7	316.6	622.1	1029	1538

The rather elementary structure of the mechanical system (beam) is the reason for the very good agreement between simulational and experimental results of modal analysis.

In the first step the transfer functions of the model (error sensor to actuator, reference sensor to actuator) are adapted automatically. Therefore, the actuators are driven with a white noise signal in a frequency range from 30 Hz to 800 Hz. The transfer functions shown in Figure 12 are determined.

Now the shaker is excited with white noise, while the adaptronical system is used to reduce the velocity amplitude of the beam. A short convergence time for the adaptive algorithm can be reached by a suitable choice of the adaptation step size α, which lies in the range of 0.4. This is lower than the upper bound described in (11) due to measurement noise. In Figure 13 the frequency responses between disturbance force and error sensor are shown, in one case controlled, and in the other case uncontrolled. Significant reductions of the amplitudes by using broadband excitation in the experiment appear. The reductions are maximal near the eigenfrequencies because there the error signals are also maximal.

Close to 200 Hz in Figure 12 an additional resonance can be observed. This is not a bending but a torsional mode excited by the huge moment of inertia of the impedance head.

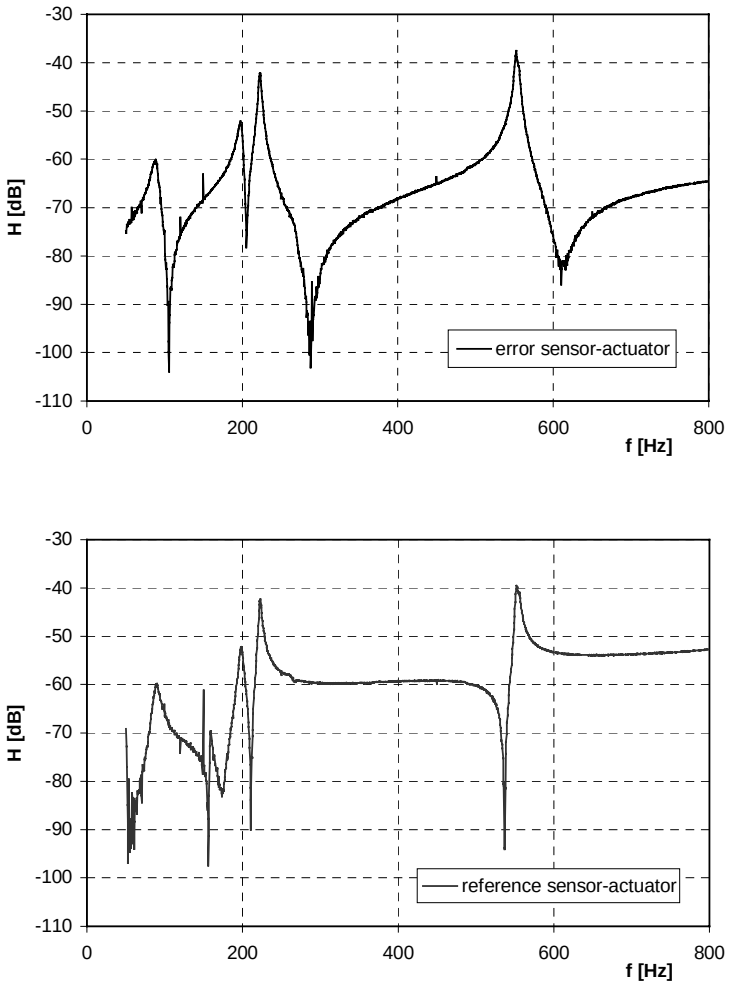

Figure 12: Transfer Functions to Establish the Internal Model of the Controller

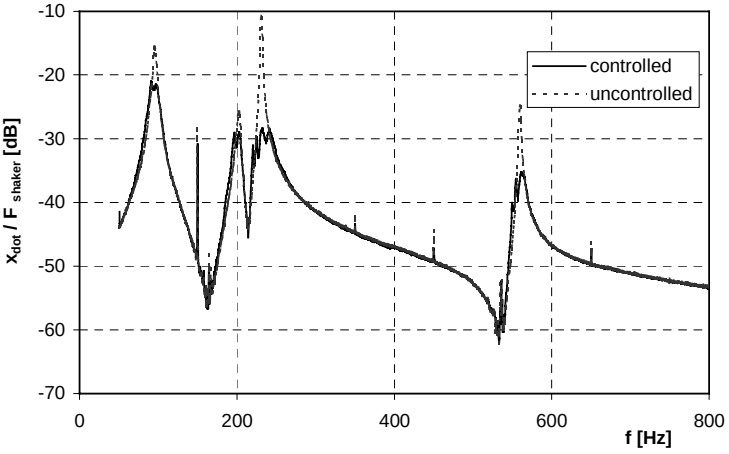

Figure 13: Frequency Responses at the Error Sensor with and without Control

6 Conclusion

A technique for the development of adaptronical systems, consisting of mechanical structure, sensors, actuators, and controller in a simulation environment has been introduced. The approach has been applied to an example of the adaptive interface for decoupling two mechanical structures with piezoceramic stack actuators. The implemented control algorithm works in the whole frequency bandwidth and allows for a good reduction of the beam vibrations. Even for the torsional eigenfrequency, which is not considered in the simulation, but occurs in the experiment, a reduction can be observed.

The presented technique will be used in further studies and extended to larger adaptronical systems. Further, the adaptive interface will be tested with other mechanical systems.

Literature

1. Bathe, K. J.: Finite Elemente Methoden, Springer Verlag, Berlin Heidelberg New York, (1990).
2. Bein, T.; Lammering, R.: Einsatzmöglichkeiten multifunktionaler Materialien im Automobilbau, VDI-Berichte Nr. 1235, (1995).
3. Fischer, U.; Stephan, W.: Mechanische Schwingungen, Fachbuchverlag Leipzig Köln, (1993).
4. Hansen, C. H.; Snyder, S. D.: Active Control of Noise and Vibration, E & FN Spon, (1997).
5. Kuo, S. M.; Morgan, D. R.: Active Noise Control Systems, Wiley & Sons Inc., New York, (1996).
6. Szabó, I.: Höhere Technische Mechanik, Springer-Verlag, Berlin Heidelberg New York, (1985).
7. Unbehauen, H.: Regelungstechnik I, Vieweg & Sohn Verlagsgesellschaft mbH, Braunschweig/ Wiesbaden, (1994).
8. Widrow, B.; Stearns, S. D.: Adaptive Signal Processing, Prentice-Hall, Inc., New Jersey, (1985).

Addresses: S. Herold, D. Mayer, University of Magdeburg, Department of Adaptronics, Universitätsplatz 2, 39106 Magdeburg, Germany; sven.herold@mb.uni-magdeburg.de, dirk.mayer@mb.uni-magdeburg.de, Prof. Dr.-Ing. H. Hanselka, Fraunhofer Institute for Structural Durability, Bartningstraße 47, 64289 Darmstadt, Germany, hanselka@lbf.fhg.de